# Evidence of two different crystalline phases of isotactic trans-1,4-poly(1,3-pentadiene). An application of the Rietveld method

**ARTICLE** *in* MACROMOLECULES · JANUARY 1986

Impact Factor: 5.8 · DOI: 10.1021/ma00155a037



**3 AUTHORS:**

Sergio Brückner
University of Udine
**110** PUBLICATIONS **2,299** CITATIONS
SEE PROFILE

di silvestro Giuseppe
University of Milan
**81** PUBLICATIONS **804** CITATIONS
SEE PROFILE

W. Porzio
Italian National Research Council
**228** PUBLICATIONS **3,030** CITATIONS
SEE PROFILE

Chem. Ed. 1981, 19, 9. (c) Mitani, K.; Ogata, T.; Nakatsukasa, M.; Eda, Y. J. Macromol. Sci., Chem. 1977, 11, 2265.
(13) Similar observations have been made by other workers; e.g., see: Palma, G.; Carenza, M. J. Appl. Polym. Sci. 1972, 16, 2485.
(14) Owen, E. D.; Pasha, I.; Moayyedi, F. J. Appl. Polym. Sci. 1980, 25, 2331.
(15) Performed by Galbraith Laboratories, Inc., Knoxville, TN.

# Evidence of Two Different Crystalline Phases of Isotactic *trans*-1,4-Poly(1,3-pentadiene). An Application of the Rietveld Method

**Sergio Brückner***

*Dipartimento di Chimica, Politecnico di Milano, 20133 Milano, Italy*

**Giuseppe Di Silvestro**

*Istituto di Chimica Industriale, Università di Milano, 20133 Milano, Italy*

**William Porzio**

*Istituto di Chimica delle Macromolecole del CNR, 20133 Milano, Italy.*
*Received May 17, 1985*

ABSTRACT: An X-ray analysis has been performed according to the Rietveld whole-fitting method on a bulk-crystallized, annealed sample of isotactic *trans*-1,4-poly(1,3-pentadiene). Calculated spectra have been obtained for different conformers in which the side methyl groups are in a cis or skew arrangement with respect to the adjacent double bonds. Comparison with the observed profile indicates that the skew conformation only gives a good agreement. This conclusion agrees with results already obtained by Neto et al. after a vibrational analysis of the same polymer. A comparison with intensities observed by Bassi et al. on an oriented fiber X-ray diagram shows however several major discrepancies. We deduce therefore the existence of two different crystalline phases that can be respectively observed in the bulk-crystallized polymer and in the sample stretched at a high temperature.

## Introduction

Bassi, Allergra, and Scordamaglia investigated the crystal structure of isotactic *trans*-1,4-poly(1,3-pentadiene) (hereafter referred to as ITPP) on the basis of the analysis of X-ray oriented fiber patterns. Their results, reported in ref 1 (hereafter paper I), clearly indicate that the conformation of the polymer chain is such that the side methyl groups are in a cis arrangement with respect to adjacent double bonds (cis model). The alternative skew arrangement (skew model), at least as stable as the former,[2] on the basis of conformational energy calculations, was rejected after many unfruitful trials to obtain an acceptable agreement with the observed intensities.

The conclusions of paper I rely indeed on a semiquantitative evaluation of observed intensities, which might induce some caution about the accuracy of the structural parameters, although the overall validity of the structural model appears to be well established. Later on Neto et al. published three papers[3-5] concerning the vibrational analysis of ITPP both in the single-chain approximation and taking into account packing effects. The results of this investigation indicate a better agreement when the skew model is adopted.

These contradictory indications prompted us to undertake a new approach to the problem, and we decided to analyze X-ray powder diffraction data of ITPP according to the Rietveld whole-fitting method.[6] Of course these experimental data would be less detailed than those of an oriented-fiber X-ray diffraction spectrum and would span a smaller $2\theta$ range, but, on the other hand, they would allow a rigorously quantitative comparison between observed and calculated intensities. Moreover with this experimental technique we had the possibility of low-temperature data recording with a consequent better signal-to-background ratio, particularly at larger $2\theta$ values.

## Experimental Section

**Sample Preparation and Characterization.** *trans*-1,4-Poly(1,3-pentadiene) was prepared by inclusion polymerization of *trans*-1,3-pentadiene in perhydrotriphenylene (PHTP) as described elsewhere.[7] The PHTP–polymer adduct was decomposed by hot extraction in boiling penthane. Inclusion polymerization of diene monomers in PHTP gives rise to a rigorously 1,4-trans enchainment as indicated by NMR data. The $^{13}C$ NMR (50.9 MHz) spectrum of the polymer shows only five peaks[8] ($\delta(C_1)$ 40.29, $\delta(C_2)$ 126.42, $\delta(C_3)$ 137.23, $\delta(C_4)$ 36.81, and $\delta(C_5)$ 19.94), which were assigned to the 1,4-trans isotactic structure. The $^{13}C$ NMR spectrum of the polymer after diimine reduction[9] shows a higher steric purity if compared with polymers synthesized in solution.[10] Low-angle X-ray scattering and superheating phenomena revealed the presence of extended chains in the paracrystalline native polymer; in particular the melting point (105 °C) and the heat of melting (116.8 J $g^{-1}$) are higher than those of the polymer annealed at 82 °C[11] (95 °C and 70.3 J $g^{-1}$, respectively). A very peculiar feature of this polymer is the extraordinary tendency toward the formation of the paracrystalline modification. In fact not only is a very slow cooling from the melt necessary in order to obtain the crystalline state,[12] but it has also been observed that if a crystalline sample is stretched at room temperature, the orientation process takes place with a simultaneous loss of crystalline order, so that the final state shows an X-ray spectrum that is typical of an oriented paracrystalline phase.[13]

**X-ray Diffraction Measurements.** For the X-ray diffraction data collection the sample holder was gradually filled by repeated evaporation from a $CHCl_3$ solution. The residual solvent was then

0024-9297/86/2219-0235$01.50/0 

**Table I**
**Experimental Details of the X-ray Diffraction Profile Measurements of Isotactic *trans*-1,4-Poly(1,3-pentadiene)**

| | |
|---|---|
| instrument | Siemens D-500 goniometer equipped with step–scan attachment, proportional counter and Soller slits, controlled with a Hewlett-Packard computer |
| radiation (power) | Cu Kα, Ni-filtered (40 kV × 30 mA) |
| divergence aperture | 0.3° from 5° to 18° (2ϑ) and 1° above (rescaling through an overlap margin of 18°–20°) |
| receiving aperture | 0.05° (2ϑ) |
| count time | 100 s per step |
| 2ϑ range | from 5° to 60° |
| temperature | +25 and −120.0 (5) °C (under vacuum ca. $10^{-3}$ mmHg) |

completely removed by keeping the sample under vacuum (0.5 mmHg) at 80 °C for ca. 2 h. The following thermal program was adopted in the annealing process: (i) 1 h at 110 °C; (ii) from 95 to 60 °C at a cooling rate of −0.002 K $min^{-1}$; (iii) from 60 °C to room temperature at a cooling rate of −0.2 K $min^{-1}$. The experimental details of intensity collection are summarized in Table I. All peaks were well interpreted, adopting the same cell dimensions ($a$ = 19.80, $b$ = 4.86, $c$ = chain axis = 4.85 Å, space group $P2_12_12_1$) of paper I. Low-temperature data (−120.0 (5) °C) were collected in order to minimize the contribution of the atomic thermal vibration parameters to the structure factors, therefore enhancing the signal-to-background ratio. Moreover the different thermal contraction along the $b$ and $c$ axes led to a significant reduction of overlapping between pairs of $hkl$ peaks related to one another by an interchange of $k$ with $l$; hence an improved experimental resolution is achieved. We refer to this resulting detailed spectrum in all comparisons with experimental data.

## Structural Analysis

A refinement routine written by Immirzi[14] was used in order to optimize nonpositional parameters (background, shape of the peaks, etc.), while the refinement of the structural models was carried out with the same routine modified by one of the authors by adding geometrical constraints in the form of Lagrange multipliers according to a computational procedure that is illustrated, e.g., in ref 15. This algorithm appears to be particularly useful in the case of polymeric models, where covalent bonding involves atoms belong to different unit cells and therefore boundary conditions must be strictly satisfied throughout the optimization process. In our analysis the 15 positional parameters of the 5 independent carbon atoms were refined under 11 constraints (5 bond lengths and 6 bond angles), thus leaving 4 effective structural degrees of freedom corresponding to the 4 torsion angles; hydrogen atoms were located at calculated positions.

The least-squares refinement is based on the minimization of $\sum_n w_n(I_{n,obsd} - I_{n,calcd})^2$ and with $w$ (the weight factor) taken as proportional to (count intensity)$^{-1}$ and on the optimization of the following quantities: (i) lattice parameters; (ii) $U$, $V$, $W$, and $m$ peak width controlling parameters; (iii) scale factor; (iv) background parameters corresponding to three bell-shaped curves plus a line connecting five points on the 2θ scale (from the observed spectrum of a quenched polymer sample; see below); (v) zero correction parameter. A convenient measure of the disagreement between observed and calculated intensities is the function $R_2' = \sum|I_o| - |I_c|/\sum I_{net}$, where $I_{net} = I_o - I_{background}$. For the sake of clarity of the following discussion it is expedient to subdivide the overall 2θ range (Cu Kα) into two regions: A ($5° \le 2\theta < 25°$ or $17.7 \le d \le 3.6$ Å) and B ($25° \le 2\theta \le 60°$ or $3.6 \le d \le 1.5$ Å); in fact, it turns out not only that region B is much more effective in discriminating between different models but also that the agreement between the observed and calculated profiles

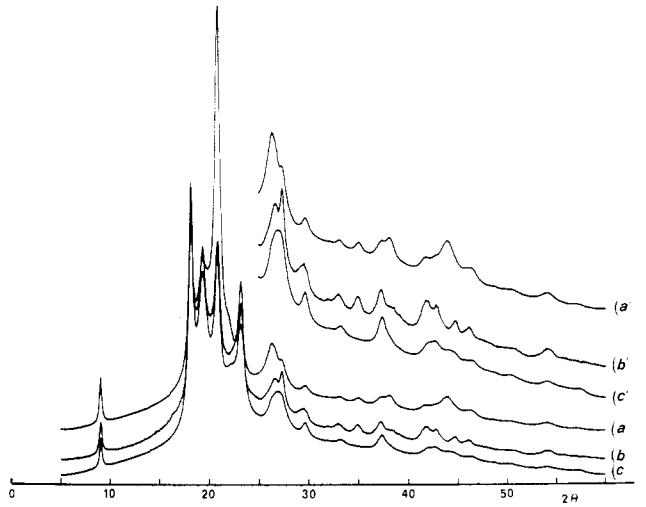


**Figure 1.** The observed X-ray diffraction profile collected at −120 °C (curve b) is compared with the profile calculated by adopting the structural cis model of paper I (curve a) and the profile that results from the same model when structural parameters are also allowed to vary in the optimization procedure (curve c). Curves a′, b′, and c′ are the same as a, b, and c but on an expanded intensity scale. The shifts of the three curves along the intensity axis are arbitrary.

**Table II**
**Comparison among the Agreements with Observed X-ray Powder Profile of the Various Structural Models Considered in the Present Work**

| | $R_2' = \Sigma\|I_o - I_c\|/\Sigma I_{net}$ | | | |
|---|---|---|---|---|
| | region A $17.7 \le d < 3.6$ Å | region B $3.6 \le d \le 1.5$ Å | total | $\chi^2/(N-P)^a$ |
| cis model (paper I)[b] | 0.60 | 0.33 | 0.51 | 61.2 |
| refined cis model (present work)[c] | 0.12 | 0.30 | 0.17 | 5.7 |
| skew model (present work)[d] | 0.11 | 0.13 | 0.12 | 2.6 |

[a] $\chi^2 = w(I_o - (1/c)I_c)^2$. $N$ = number of profile points; $P$ = total number of refined parameters; $1/c$ = scale factor; $w$ = weight factor. [b] Refinement performed on structural parameters only. [c] Curve c in Figure 1. [d] Curve d in Figure 1.

in this region is almost independent from the actual choice of the background parameters used to describe the three bumps of the base line.

The results of paper I were first used, without any modification of the structural model, to obtain a diffraction profile to compare with experimental data obtained both at room temperature and at −120 °C. This comparison is shown in Figure 1, where curve a is the calculated profile and curve b is the observed one at −120 °C. The two curves show several points in disagreement; in particular the peak corresponding to reflection 210 (and 201) at $2\theta = 20.8°$ is calculated as more than twice as strong as the observed one. A summary of the disagreement factors for this and other models is reported in Table II. A few cycles of structural refinement however were sufficient to eliminate this striking feature without involving dramatic changes among the positional parameters, so that the resulting model (refined cis model) was still acceptable from the point of view of packing distances. However, as summarized in Table II, the agreement in region B did not improve significantly, as may also be seen in Figure 1, where curve c refers to this refined cis model. The refinement of the cis model led also to some major discrepancies with

**Table III**
**Summary of the Major Discrepancies Detected by Comparing Intensities Calculated with Models Refined on the Powder X-ray Spectrum with Intensities Observed on the Oriented Fiber Spectrum (Reported in Paper I)**

| | | intensities | | | |
|---|---|---|---|---|---|
| *hkl* | 2$\vartheta$, deg | obsd (paper I) | cis model[a] (paper I) | refined cis model (present work) | skew model (present work) |
| 310 | 23.2 | ms | 398 | 1274 | 1227 |
| 610 | 33.3 | vvw | 3 | 68 | 3 |
| 220 | 39.0 | vvw | 5 | 26 | 68 |
| 520 | 44.6 | vw | 41 | 187 | 71 |
| 11,1,0 | 55.1 | | 1 | 40 | 24 |
| 101 | 18.8 | mw | 185 | 40 | 299 |
| 201 | 20.4 | m | 156 | 439 | 10 |
| 301 | 22.8 | m | 128 | 53 | 506 |
| 221 | 43.4 | mw | 128 | 79 | 11 |
| 621 | 51.1 | | 1 | 32 | 30 |
| 821 | 57.3 | vw | | | |
| 11,1,1 | 58.5 | vw | 27 | 24 | 117 |
| 512 | 48.0 | | 5 | 50 | 106 |
| 802 | 53.0 | | 1 | 3 | 46 |
| 222 | 54.8 | | 1 | 34 | 32 |
| 522 | 59.3 | | 14 | 25 | 64 |

[a] Calculated intensities from paper I are also reported in order to give a numerical basis for comparison.

the observed data on the oriented-fiber X-ray spectrum; as an example, reflection 201 is calculated as about 10 times as strong as 101 and 301, while in paper I these three reflections are observed (and calculated) with approximately the same intensity. A brief summary of the largest disagreements with the observed fiber diagram for this and for the skew model is reported in Table III.

Further trials in testing the cis model were attempted, among which one of the most acceptable for packing was performed on a structure derived from that of paper I through a reflection of the macromolecule by a noncrystallographic mirror plane parallel to the *c* axis and approximately containing the main-chain axis and the side methyl group. All these attempts resulted in a worse agreement between observed and calculated profiles. It was clear that the cis model, though valid in explaining the oriented-fiber X-ray pattern, was unable to account for the diffraction from the bulk-crystallized sample as well. The skew model was then taken into account and its orientation within the unit cell adjusted in order to locate the side methyl group at the same position occupied in the case of the cis model. In fact the overall shape of the polymer chain in both conformational models may be roughly described in terms of a rod with periodic side bumps, and it can be assumed that packing is substantially determined by the relative positions of these bumps. Refinement of the skew model led to a satisfactory agreement both in region A and in region B as can be seen in Table II and in Figure 2, where observed and calculated profiles are compared through the whole 2$\theta$ range. A comparison between intensities calculated with the skew model and observed on the oriented fiber diagram revealed again many disagreements, some of which are reported in Table III. As an example, in this case, reflection 201 is calculated as very weak while, as previously stated, it is observed in the fiber diagram as a well-resolved medium-intensity peak. Concerning the particularly complex background curve (see Figure 2), we tested its reliability by quenching the melted sample and recording the X-ray diffraction profile at −120 °C. We obtained a curve very similar to the background curve of Figure 2 with the bumps clearly visible at the same 2$\theta$ values.

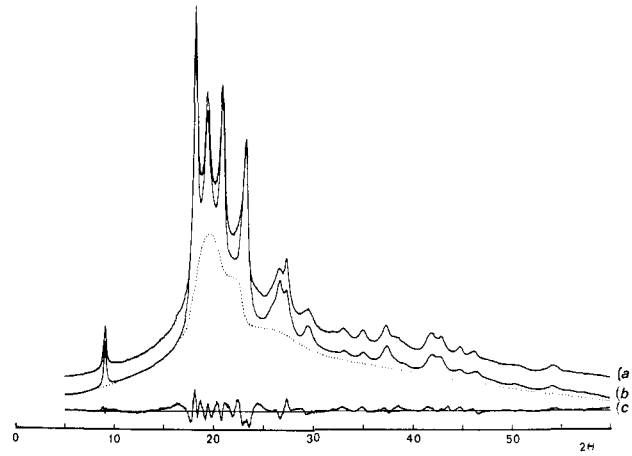


**Figure 2.** The observed X-ray diffraction profile collected at −120 °C (curve a) is compared with the profile calculated by adopting the structural skew model (curve b). The dotted curve indicates the calculated background profile while curve c represents the difference profile.

**Table IV**
**Structural Parameters of the Conformational Model with the Side Methyl Group in Skew Arrangement with Respect to the Nearest Double Bond (Skew Model)**

| | *x* | *y* | *z* | *B* (Å$^2$ at −120 °C) |
|---|---|---|---|---|
| C(1) | 0.1143 (2) | 0.1842 (9) | −0.1907 (10) | 0.1 |
| C(2) | 0.1104 (2) | 0.0198 (10) | 0.0718 (10) | 0.1 |
| C(3) | 0.0881 (2) | 0.1507 (9) | 0.2994 (9) | 0.1 |
| C(4) | 0.0875 (2) | −0.0028 (10) | −0.4268 (9) | 0.1 |
| C(5) | 0.1893 (2) | 0.2661 (9) | −0.2416 (9) | 0.1 |
| H(1) | 0.0831 | 0.3736 | −0.1743 | 1 |
| H(2) | 0.1257 | −0.2059 | 0.0779 | 1 |
| H(3) | 0.0704 | 0.3669 | 0.2876 | 1 |
| H(4) | 0.0353 | −0.0662 | −0.3800 | 1 |
| H(5) | 0.1197 | −0.1892 | −0.4427 | 1 |
| H(6) | 0.2186 | 0.2366 | −0.0534 | 1 |
| H(7) | 0.1921 | 0.4861 | −0.3043 | 1 |
| H(8) | 0.2105 | 0.1335 | −0.4032 | 1 |

Bond Lengths, Å

| | | | |
|---|---|---|---|
| C(1)–C(2) | 1.50 (1) | C(1)–C(5) | 1.54 (1) |
| C(2)–C(3) | 1.34 (1) | C(1)–C(4) | 1.54 (1) |
| C(3)–C(4)′ | 1.52 (1) | | |

Bond Angles, deg

| | | | |
|---|---|---|---|
| C(1)–C(2)–C(3) | 118.6 (5) | C(1)–C(4)–C(3)′ | 112.0 (5) |
| C(2)–C(3)–C(4)′ | 120.3 (5) | C(2)–C(1)–C(5) | 108.6 (5) |
| C(2)–C(1)–C(4) | 108.6 (5) | C(4)–C(1)–C(5) | 110.5 (5) |

Torsion Angles, deg

| | | | |
|---|---|---|---|
| C(1)′–C(4)′C(3)–C(2) | 136 (1) | C(3)–C(2)–C(1)–C(5) | 102 (1) |
| C(4)′–C(3)–C(2)–C(1) | −176 (1) | C(2)–C(1)–C(4)–C(3)′ | 178 (1) |
| C(3)–C(2)–C(1)–C(4) | −138 (1) | | |

During the last steps of the refinement procedure the geometrical constraints on the model were slightly relaxed in order to improve agreement with the observed data. The deviations of internal coordinates were all within an acceptable range, as can be seen in Table IV, where the geometry of the skew model is summarized. A last adjustment was performed, by trials, on the torsion angle of the bond connecting the side methyl group to the main chain, setting the best value at −50 °C (close to the staggered conformation). The overall isotropic thermal parameter was not refined since a strong correlation exists with the scale factor, which, in turn, is strongly affected by background parameters, particularly by the bell-shaped curves; its low value, 0.1 Å$^2$ for all carbon atoms at −120 °C (and 1 Å$^2$ for all hydrogen atoms), is therefore to be considered only indicative and unworthy of a detailed discussion. A summary of the final values of nonstructural

Table V
Refined Nonstructural Parameters for the Skew Model

| | |
|---|---|
| zero correction $2\vartheta$, deg | −0.037 (7) |
| profile function parameters[a] | |
| $U$ | 5.68 (85) |
| $V$ | 1.00 (24) |
| $W$ | −0.038 (28) |
| $m$ | 1 |
| background intensities (K counts) | |
| $2\vartheta$ = 5.0° | 0.200 (8) |
| $2\vartheta$ = 20.5° | 0.905 (16) |
| $2\vartheta$ = 30.0° | 0.875 (15) |
| $2\vartheta$ = 42.0° | 0.502 (5) |
| $2\vartheta$ = 60.0° | 0.118 (3) |

Bell-Shaped Curves[b]

| no. | int/1000 | width, deg | $2\vartheta$, deg |
|---|---|---|---|
| 1 | 0.349 (9) | 2.04 (6) | 19.6 (7) |
| 2 | 0.068 (5) | 1.50 (5) | 22.0 (5) |
| 3 | 0.202 (7) | 3.50 (8) | 26.1 (8) |

Direct Lattice Constants,[c] Å

| | +25 °C | −120 °C |
|---|---|---|
| $a$ | 19.802 (13) | 19.587 (9) |
| $b$ | 4.801 (8) | 4.749 (5) |
| $c$ | 4.850 (8) | 4.860 (5) |

[a] According to the relation $2H_k = U \tan^2 \vartheta_k + V \tan \vartheta_k + W$; $m$ is the exponent in the Pearson profile function $f(z) = (C/H_k)[1 + 4(2^{1/m} - 1)z^2]^{-m}$ with $z = (2\vartheta_i - 2\vartheta_k)/H_k$. [b] The bell-shaped curves have again the form of a Pearson peak with $m = 1$. [c] Space group $P2_12_12_1$. Calculated from the squared reciprocal constants.

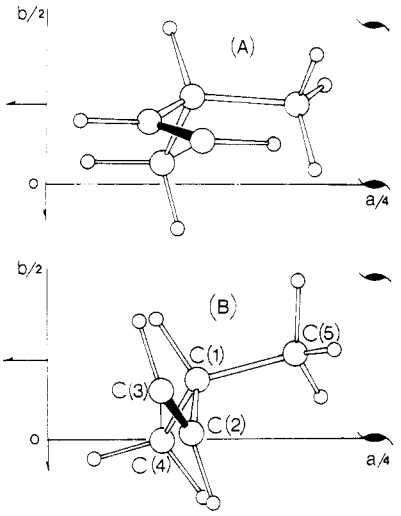


**Figure 3.** A comparison between the cis model of paper I (A) and the skew model of the present work (B). Both models are represented in their actual position within the unit cell.

parameters resulting from the refinement of the skew model is reported in Table V.

The conformation of the polymer chain may be described as a sequence of $S^+TS^-T$ rotations, where the symbols T and $S^{\pm}$ refer respectively to the trans and the two enantiomorphous skew conformations. Their values, +136 (1)° and −138 (1)°, deviate significantly from the theoretical value of ±120°, but this is not surprising since such strong deviations have been already observed in low molecular weight models, as is summarized in Table 7 of ref 16. A visual comparison between the cis model of paper I and the skew model of the present work is shown in Figure 3, where it is also possible to see the position occupied by the two models within the unit cell. It may be seen that while the carbon atoms of the side methyl groups are almost superimposable, the main-chain axes undergo a small shift along $b$. The most significant packing distances are shown in Figure 4, and it may be seen that also for the presently proposed model none of them is shorter than 4 Å, in agreement with the previous assumption that the location of the side methyl group is the most critical feature affecting the packing of these macromolecules.

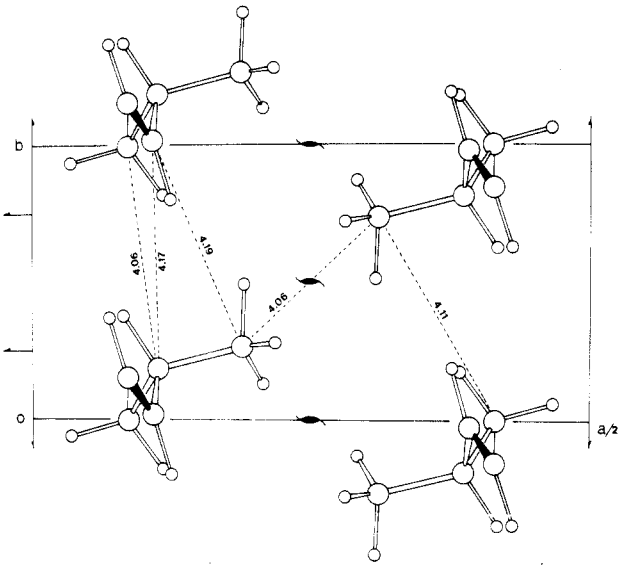


**Figure 4.** Packing of the macromolecules of isotactic *trans*-1,4-poly(1,3-pentadiene) in the crystalline state.

## Concluding Remarks

It seems quite clear that experimental data obtained by X-ray diffraction from an oriented fiber and from a bulk-crystallized sample cannot be explained by the same structural model. We can conclude therefore that stretching a sample of crystalline IPTT at a temperature just below the melting point (95 °C) gives rise to an oriented crystalline phase that is different from that obtained by simply annealing the sample in the absence of any perturbing mechanical stress. This conclusion also explains the disagreement between the results of Neto et al., obtaied by analyzing an unstretched sample, and the X-ray structure proposed from the oriented fiber diagram in paper I. The cell parameters of the two crystalline forms are the same within experimental error; in particular, no significant difference is detected along the chain axis. This observation prevents any simple hypothesis about the mechanism by which stretching induces the conformational change. It is worth pointing out, however, that the coexistence of different conformers within the same cell, at increasing temperature, cannot be rejected "a priori"; in fact intramolecular energy, conformational analysis,[2] and experimental findings[16-18] indicate that the two conformations involve a small energy difference, while packing contacts are dominated by interactions of the side methyl groups, whose distance from the main-chain axis is only slightly longer (0.25 Å) in the skew model. If this is the case, we must deduce that stretching at higher temperature has the effect of favoring the prevailing presence of the cis conformer within the crystal lattice. Further investigation is required on this subject, which is also likely to be related to the extraordinary stability of the paracrystalline phase of ITPP.

**Acknowledgment.** We thank Prof. G. Allergra, Dr. G. Perego, and Dr. P. Sozzani for helpful discussion and suggestions. This work has been partially supported by a grant by Ministero della Pubblica Istruzione, Italy, and by the Progetto Finalizzato per la Chimica Fine e Secondaria, CNR, Italy.

**Registry No.** Isotactic *trans*-poly(1,3-pentadiene) (homopolymer), 29191-23-9.

## References and Notes

(1) Bassi, I. W.; Allegra, G.; Scordamaglia, R. *Macromolecules* **1971**, *4*, 575.
(2) Mark, J. E. *J. Am. Chem. Soc.* **1967**, *89*, 6829.
(3) Neto, N.; Muniz-Miranda, M.; Benedetti, E.; Garruto, F.; Aglietto, M. *Macromolecules* **1980**, *13*, 1295.
(4) Neto, N.; Muniz-Miranda, M.; Benedetti, E. *Macromolecules* **1980**, *13*, 1302.
(5) Neto, N. *Kem. Kozl.* **1982**, *57*, (3–4), 259.
(6) Young, R. A.; Mackie, P. E.; Von Dreele, R. B. *J. Appl. Crystallogr.* **1977**, *10*, 262; see also references cited therein.
(7) Farina, M.; Pedretti, U.; Gramegna, M. T.; Audisio, G. *Tetrahedron* **1970**, *26*, 1839.
(8) Sozzani, P.; Di Silvestro, G.; Grassi, M.; Farina, M. *Macromolecules* **1984**, *17*, 2532.
(9) Mango, L. A.; Lenz, R. W. *Makromol. Chem.* **1973**, *163*, 13.
(10) Zetta, L.; Gatti, G.; Audisio, G. *Macromolecules* **1978**, *11*, 763.
(11) Farina, M.; Di Silvestro, G. *Makromol. Chem.* **1982**, *183*, 241.
(12) Natta, G.; Porri, L.; Gorradini, P.; Zanini, C.; Ciampelli, F. *J. Polym. Sci.* **1961**, *51*, 463.
(13) Perego, G., private communication.
(14) Immirzi, A. *Acta Crystallogr., Sect. A.: Cryst. Phys., Diffr., Theor. Gen. Crystallogr.* **1978**, *A34*, S-348.
(15) Tadokoro, H. In "Structure of Crystalline Polymers"; Wiley: New York, 1979.
(16) Martuscelli, E. *Acta Crystallogr., Sect. B: Struct. Crystallogr. Cryst. Chem.* **1969**, *B25*, 2540.
(17) Martuscelli, E.; Frasci, A. *Acta Crystallogr., Sect. B: Struct. Crystallogr. Cryst. Chem.* **1969**, *B25*, 2547.
(18) Corradini, P.; Frasci, A.; Martuscelli, E. *Chem. Commun.* **1969**, 778.